Theor Chem Account (2009) 122:245–256
DOI 10.1007/s00214-009-0508-1

REGULAR ARTICLE

Theoretical conformational study of six-membered cyclic allyl epoxides

Paolo Crotti · Valeria Di Bussolo · Christian Silvio Pomelli · Lucilla Favero

Received: 11 September 2008 / Accepted: 17 December 2008 / Published online: 14 February 2009

Abstract Accurate "ab initio" calculations (MP2 method) were performed to outline the conformational profile of a number of six-membered cyclic allyl epoxides differing either in the nature of the cycle fragment (Y) bound to the unsaturation, or in the substitution at the endocyclic carbon bound to the epoxy ring and bridging the epoxy ring with the Y fragment. In particular, we calculated structures **4** (Y=CH_2), **5** (Y=O), **6** (Y=NH), **7** (Y=S), **8** (Y=CF_2), **9** (Y=NH_2^+), **10** (Y=CO), **11** (Y=BH) and **12** (Y=NCOOH), where the fragment of the endocyclic carbon bridging "Y" and the epoxy fragment is either non-substituted (**4a**–**12a**) or bears a methyl side chain *trans* (**4b**–**12b**) or *cis* (**4c**–**12c**) to the epoxidic oxygen. Saturated analogs (Y=O and Y=CH_2) were also computed to test the method and to evaluate the conformational profile in the absence of the unsaturation. Minimum energy conformations were found which differ in the relative position of the Y group and the epoxy oxygen, with respect to a plane containing the epoxy ring carbons and the adjacent saturated endocyclic carbon: they may be on the same side (conformer **A**) or on opposite sides (conformer **B**). Conformers **A** are generally more stable. The conjugation effect of Y with the double bond lowers the barrier between the two conformers to the extent that in a few cases only conformer **A** is associated with a minimum of energy. On the basis of the elongation of the allylic oxirane C–O bond, we postulated the order of reactivity of epoxides **4**–**12** in the oxirane ring-opening process, and a mechanism based on the more reactive conformer **A**. A comparison was also made between MP2 and DFT calculation methods.

Keywords Conformational study · Allyl epoxides · Reactivity · MP2-DFT

1 Introduction

Allyl epoxides are valuable synthetic intermediates undergoing addition of nucleophiles with high stereo- and regiochemical control to provide unsaturated compounds amenable in turn to further stereoselective elaboration [1]. In this connection, we recently found that diastereoisomeric D-galactal, D-allal and *N*-benzyloxycarbonyl-imino (*N*-Cbz-imino) glycal-derived allyl epoxides (epoxides **1α** and **1β**, as an example) undergo highly stereoselective glycoside bond formation by 1,4 addition of *C*- or *O*-nucleophiles, to yield 2-unsaturated glycosides (pseudoglycals) (Scheme 1) [2–5]. These compounds can be further regio- and stereoselectively functionalized at the double bond, to provide oligosaccharides which would be difficult to obtain by direct glycosylation of the appropriate mono- or oligosaccharides [6–9]. The approach could be in principle applied to glycoside analogs in which the endocyclic oxygen is replaced by another group such as CH_2, CF_2, C=O, S, N–*R*.

Conformational analysis is normally the starting-point in the prediction or rationalization of the regio- and

Electronic supplementary material The online version of this article (doi:10.1007/s00214-009-0508-1) contains supplementary material, which is available to authorized users.

P. Crotti · V. Di Bussolo · L. Favero (✉)
Dipartimento di Scienze Farmaceutiche
(Chimica Bioorganica e Biofarmacia),
via Bonanno, 33, Pisa, Italy
e-mail: lucillaw@farm.unipi.it

C. S. Pomelli
Dipartimento di Chimica e Chimica Industriale,
via Risorgimento 35, Pisa, Italy

Scheme 1 Route of glycal-derived epoxides to glycosides

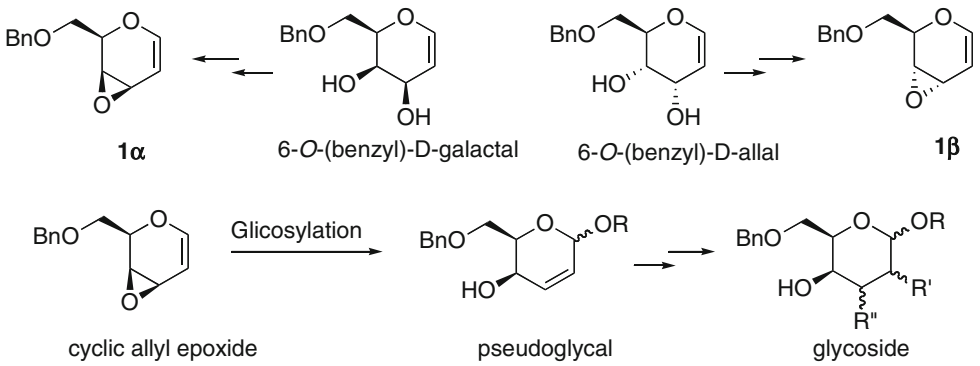

stereochemical outcome of reactions in a cyclic system, but in the case of heterocyclic allyl epoxides, steric and stereoelectronic factors, strain and conjugation combine in such a complex way that traditional conformational analysis, as well as molecular mechanics, cannot be reliably applied. In order to provide an accurate description of the ground states of a number of potentially useful heterocyclic allyl epoxides, and single out different factors contributing to the complete conformational profile, we decided to investigate structures **4**–**12** (Fig. 1), by means of the "ab initio" MP2 method and to outline how a number of molecular factors (dipole moment, torsional, steric and electronic effects) affect conformations. One further reason for performing these calculations is that the allyl epoxides are in many cases (Y=O, Y=*N*-Cbz) not stable enough to allow accurate conformational analysis by spectroscopic methods.

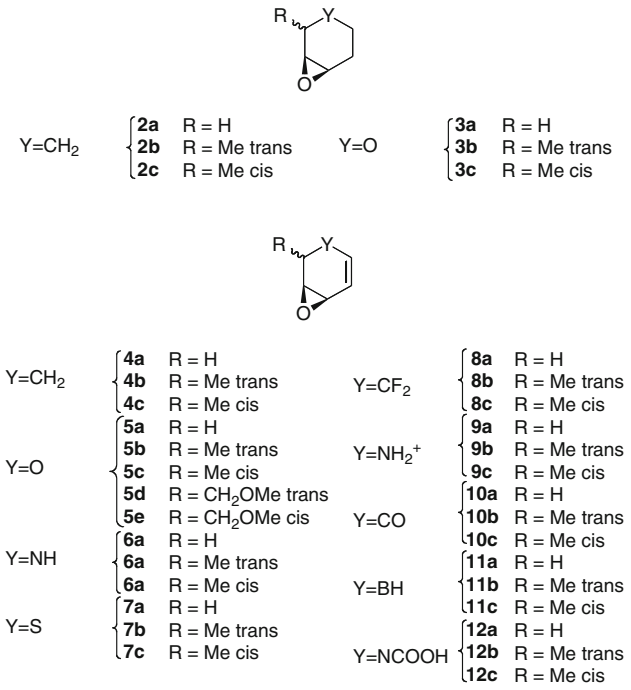

Fig. 1 Epoxides derived from six-membered cyclic systems

As can be seen, structures 4–12 differ in the nature of the "Y" fragment of the cycle bound to the unsaturation. "Y" was allowed to vary among groups with different electronic demands, they include: saturated groups with different inductive effect such as CH_2, CF_2 and NH_2^+ (compounds **4**, **8** and **9**, respectively); electron-deficient groups such as BH and C=O (compounds **10** and **11**, respectively); electron-rich groups such as O, NH, S and NCOOH (**5**, **6**, **7** and **12**, respectively). For each cyclic structure indicated above, we considered cases in which the carbon atom [C(5)] bridging "Y" and the epoxy fragment is unsubstituted (**4a**–**12a**), and those in which a methyl side chain is present *trans* (**4b**–**12b**) or *cis* (**4c**–**12c**) with respect to the epoxy oxygen atom. The methyl group was expected to adequately model the benzyloxymethyl group (CH_2OBn) present in pyrane-based allyl epoxides (epoxides **1α** and **1*β***, for example) typically involved in oligosaccharide chemistry. The methyl group has the advantage of being less demanding from the point of view of computing, and free from the complications due to the presence of rotamers generated by rotation around the bonds of the $-CH_2OBn$ group. The validity of this assumption was confirmed by comparison of data obtained for methyl- and methoxymethyl-substituted analogs of the pyran series **5**. In order to test the computational method by comparison of results with experimental data available for conformers ratio, and also to evaluate the specific effect of the molecular factors on conformational profiles in the absence of the unsaturation, we also preliminarily computed saturated carbocyclic epoxides **2** and pyran epoxides **3** (Fig. 1).

On the basis of the results of ground state calculations, we also propose here a mechanistic interpretation of the reactivity of compounds **4**–**12**. In particular, we suggest that the order of reactivity in the addition of nucleophiles to allyl epoxides **4**–**12** is related to the extent to which "Y" affects allylic C–O bond elongation, and we postulated a mechanism for the reaction, which is based on the more reactive conformer.

A comparison between the MP2 and B3LYP calculation methods was also made in order to test the reliability of the less CPU-expensive DFT method in the computation of the above-described molecular systems. The applicability of DFT is also important in view of MD simulations, for which MP2 is not applicable.

1.1 Computational details

Quantum-chemical computations were carried out with the Gaussian 03 package [10]. The calculations were performed using the perturbative MP2 frozen core (FC) method [11–15]. The less CPU-expensive DFT method (B3LYP) [16] was checked to see if it was suitable for this family of compounds. Where not otherwise indicated in the text, 6-31+G(d) [17] was used as the basis set. Both MP2 and B3LYP methods were used to perform the relaxed scan (by optimizing all other internal coordinates) on the PES around the dihedral $\boldsymbol{\theta_1}$ (H–C(4)–C(5)–R^2), involved in the conformational interconversion of the saturated (**2–3**) and allyl epoxides (**4–12**). Berny analytical gradient optimization routines [18] were used for optimization of the stationary points (**TS**s and minima) on the PES. The Berny algorithm was used to locate the transition structures (**TS**s). All stationary points were characterized by frequency calculations, in order to verify that minima and **TS**s have no or only one imaginary frequency. We also performed for all the structures the MP2/6-31+G(d) SP (single point) energy calculations on the previously B3LYP/6-31+G(d) optimized structures, in order to compare the results obtained with the ones provided by a full MP2 optimization. In the most interesting case of epoxide **5**, both CCSD (frozen core FC) [19] and MP4 (frozen core FC) [20, 21] SP on the previously optimized MP2 structure, and full CCSD (FC) optimization were also performed.

Unless otherwise indicated, NBO analysis was performed using the generalized density obtained at the MP2/6-31+G(d) level. Enthalpy, entropy, ZPE and Gibbs free energy values were calculated using the standard expressions for an ideal gas in the canonical ensemble at 298.15 K and 1 atm pressure [22]. For all structures, the calculated Gibbs free energy values in the gas phase (vacuum) were corrected by adding the ZPE and taking away E-TS rotational and translational terms. These thermal and entropic corrections were calculated in accordance with the Ben-Naim scheme for thermochemical properties in the liquid phase [23]. The IEF-PCM [24–28] model [atomic radii: simple united atom topological model (UAO)] was used to include the solvent (methanol or benzene) in order to examine its influence on the conformational population for the epoxides **3a**, **5a–e**, **8a** and **9a**.

2 Results and discussion

The results of our calculation (ΔG between minimum energy conformations and $\Delta G^{\ddagger}$ for interconversion barrier) for epoxides **2–12**,[1] are summarized in Table 1.[2] In most cases, two minimum energy conformations were found, differing in the relative position of the Y group and the epoxy oxygen, with respect to a plane containing the epoxy ring carbons C(3)–C(4) and the adjacent saturated endocyclic carbon C(5): in one conformer (conformer **A**) they are on the same side of the plane and in the other conformer (conformer **B**) they are on opposite sides (Scheme 2).

In saturated epoxides **2–3**, the conformational equilibrium seems to be principally affected by two factors: the dipole moment difference between the two conformers and the position of the side chain, when present. In the case of epoxide **3a**, torsional effects in the two conformers **A** and **B** are practically identical, as in the case of the degenerate conformers **2a-A** and **2a-B**. The lower free energy associated with conformer **3a-B** (1.36 kcal/mole) and the resulting equilibrium ratio (**3a-B**:**3a-A** = 91:9, entry 4a) has been explained in terms of the repulsion between the dipoles associated with the endocyclic and oxirane oxygen atoms [31]. In agreement with this explanation, we found that the lower-energy conformer **B** has a lower dipole moment ($|\mu\mathbf{A}| - |\mu\mathbf{B}| = 2.05$, entry 4a). As expected, solvents of higher polarity shift the equilibrium ratio in favor of the more polar conformer **A** (entries 4b–c).

The presence of a methyl group at C(5) has a marked effect on the conformational profile of **2** and **3**, but it can only be explained on the basis of steric effects, because the $\Delta\mu$ values of conformers seem to be insensitive to alkyl substitution at C(5) (entries 2, 3 and 5a, 6a). The substituents have an obvious preference for the equatorial position; as a consequence, while the presence of the methyl group *trans* to the epoxide oxygen (**3b**) enhances the ΔG between conformers **A** and **B** (**3b-B**:**3b-A** = >99:<1, entry 5a), in the diastereoisomer epoxide **3c**, the methyl group *cis* to the epoxide oxygen lowers the ΔG between conformers **A** and **B** (**3c-B**:**3c-A** = 38:62, entry 6a, Table 1) [32]. The preference for the equatorial location seems to have a stronger effect on the ΔG value in the case of the pyranic epoxides **3b** and **3c**, where the variations are 1.99 and 1.64 kcal/mol, respectively, than in the case of the cyclohexane epoxides **2b** and **2c**, where the preference for the conformer bearing the equatorial methyl group is 1 kcal/mol (entries 2 and 3, Table 1). It is appropriate to mention here that, for the

[1] Obviously, for cyclohexene oxide **2a** conformer **A** is equivalent to conformer **B** (entry 1, Table 1).

[2] The corresponding potential energy values ΔE and $\Delta E^{\ddagger}$ are reported in Table S4, ESM.

Table 1 MP2/6-31+G(d) data (kcal/mol) relative to the conformational interconversion for epoxides **2–12**

Entry	Y	Y hybrid[a]	(**A**) ⇌ (**B**) interconversion	Δμ (D) (μ**A**-μ**B**)	ΔG^{b}	% (**B**:**A**)	$\Delta G^{\ddagger b}$
1[c]	CH_2	*sp³-like*	**2a-A** ⇌ **2a-B**[d]	0.0	0.00	50:50	+5.08
2[e]			**2b-A** ⇌ **2b-B**[f]		−1.01	85:15	+4.92
3[e]			**2c-A**[f] ⇌ **2c-B**		+1.04	15:85	+5.19
4a	O	*sp²-like*	**3a-A** ⇌ **3a-B**	+2.1	−1.36	91:9	+6.27
4b[g]			**3a-A** ⇌ **3a-B**		−1.07	86:14	
4c[h]			**3a-A** ⇌ **3a-B**		+0.24	40:60	
4d[i]			**3a-A** ⇌ **3a-B**		−0.82 ± 0.12	80:20	
5a			**3b-A** ⇌ **3b-B**		−3.35	>99:<1	+4.99
5b[j]			**3b-A** ⇌ **3b-B**		…	>99:<1	
6a			**3c-A** ⇌ **3c-B**		+0.28	38:62	+6.38
6b[j]			**3c-A** ⇌ **3c-B**		+0.24 ± 0.12	40:60	
7[k]	CH_2	*sp³-like*	**4a-A** ⇌ **4a-B**	−0.4	+3.21	1:99	+4.95
8			**4b-A** ⇌ **4b-B**		+2.91	1:99	+5.67
9			**4c-A** ⇌ **4c-B**		+4.40	>99:<1	+5.83
10a	O	*sp²-like*	**5a-A** ⇌ **5a-B**	+1.2	+0.84	19:81	+1.44
10b[g]			**5a-A** ⇌ **5a-B**		+0.99	16:84	
10c[h]			**5a-A** ⇌ **5a-B**		+1.44	8:92	
11a			**5b-A** ⇌ **5b-B**		+0.29	38:62	+1.53
11b[g]			**5b-A** ⇌ **5b-B**		+0.52	29:71	
11c[h]			**5b-A** ⇌ **5b-B**		+1.16	12:88	
12			**5c-A** ⇌ **5c-B**		Only **A**[l]		
13a			**5d-A** ⇌ **5d-B**			32:68[m]	
13b[g]			**5d-A** ⇌ **5d-B**			18:82[m]	
13c[h]			**5d-A** ⇌ **5d-B**			>99:<1[m]	
14			**5e-A** ⇌ **5e-B**		Only **A**[l,m]		
15	NH	*sp²-like*	**6a-A** ⇌ **6a-B**	+0.5	+1.09	14:86	+1.41
16			**6b-A** ⇌ **6b-B**		+0.62	26:74	+1.21
17			**6c-A** ⇌ **6c-B**		Only **A**		
18	S	*sp²-like*	**7a-A** ⇌ **7a-B**	+1.7	+0.96	17:83	+2.73
19			**7b-A** ⇌ **7b-B**		+0.75	22:78	+3.39
20			**7c-A** ⇌ **7c-B**		+2.19	2:98	+3.25
21a	CF_2	*sp²-like*	**8a-A** ⇌ **8a-B**	+2.5	+1.05	15:85	+3.24
21b[g]			**8a-A** ⇌ **8a-B**		+1.33	10:90	
21c[h]			**8a-A** ⇌ **8a-B**		+2.08	3:97	
22			**8b-A** ⇌ **8b-B**		+0.75	22:78	+4.82
23			**8c-A** ⇌ **8c-B**		+1.76	5:95	+4.89
24a	NH_2^+	*sp³-like*	**9a-A** ⇌ **9a-B**	−2.0	+7.17	>99:<1	+9.23
24b[g]			**9a-A** ⇌ **9a-B**		+5.68	>99:<1	
24c[h]			**9a-A** ⇌ **9a-B**		+3.30	>99:<1	
25			**9b-A** ⇌ **9b-B**		+6.60	>99:<1	+9.58
26			**9c-A** ⇌ **9c-B**		+7.62	>99:<1	+9.37
27	C=O	*sp²-like*	**10a-A** ⇌ **10a-B**	Only **A**			
28			**10b-A** ⇌ **10b-B**	Only **A**			
29			**10c-A** ⇌ **10c-B**	Only **A**			
30	BH	*sp²-like*	**11a-A** ⇌ **11a-B**	Only **A**			
31			**11b-A** ⇌ **11b-B**	Only **A**			
32			**11c-A** ⇌ **11c-B**	Only **A**			

Table 1 continued

Entry	Y	Y hybrid[a]	(**A**) ⇌ (**B**) interconversion	Δμ (D) (μ**A**-μ**B**)	ΔG^{b}	% (**B**:**A**)	$\Delta G^{\ddagger b}$
33	NCOOH	*sp²-like*	**12a-A** ⇌ **12a-B**	Only **A**			
34			**12b-A** ⇌ **12b-B**	Only **A**			
35			**12c-A** ⇌ **12c-B**	Only **B**			

[a] Obtained by NBO analysis

[b] The free energy values calculated in a vacuum (all entries except 4b–c, 10b–c, 11b–c, 13b–c, 21b–c and 24b–c) were corrected by adding the ZPE and taking away E-TS rotational and translational terms [23]

[c] See [29]

[d] See footnote 1

[e] See [30]

[f] Conformer having the side chain in the equatorial position

[g] Results obtained in benzene

[h] Results obtained in methanol

[i] Experimental results (benzene and $CHCl_3$): see [31]

[j] Experimental results (benzene and $CHCl_3$): see [32]

[k] See [33]

[l] The same result was obtained also in the presence of a solvent (benzene or methanol)

[m] All the rotamers (three for each conformer) around the C(5)-CH_2OMe bond in the side chain were also considered (see Figure S3 and Table S6, ESM)

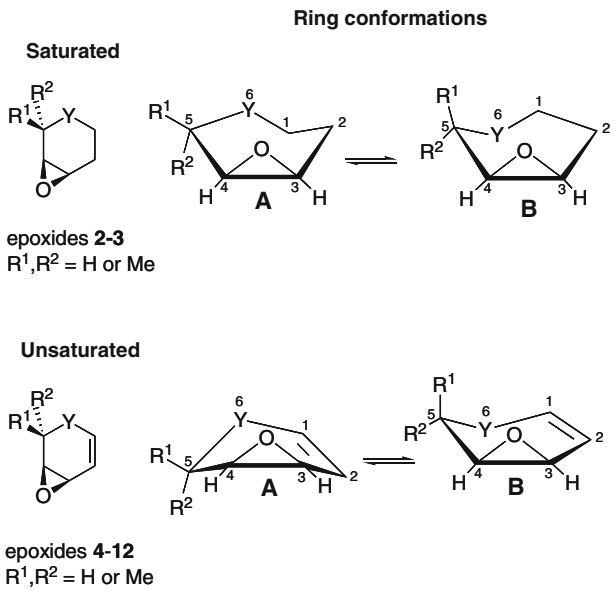

Scheme 2 Conformational equilibrium of epoxides **2**–**12**

equilibrium ratio of epoxides **3a**–**c**, experimental ΔG values are available, based on ^{1}H NMR studies [31, 32] (entries 4d, 5b and 6b, Table 1). The close agreement between the MP2 ΔG and the corresponding experimental data, found for epoxide **3a**–**c**, is a validation of our calculation method.

With unsubstituted allyl epoxides **4a**–**12a**, regardless of the nature of "Y", conformers **A** are generally the preferred ones, and in a few cases (epoxides **10a**–**12a**, entries 27, 30 and 33) they are the only conformers associated with a minimum energy. The interactions of the "Y" group with the unsaturation are mainly responsible for the effects on the conformational profile in terms of ΔG, $\Delta G^{\ddagger}$ and the number of energy minima.

Except for derivatives **4a** and **9a** (Y=CH_2 and NH_2^+, respectively), in which the endocyclic atom of the Y group is clearly an sp^3 hybridized atom (as evaluated by NBO analysis), the ΔG between the two conformers is unvaried with respect to Δμ (entries 10a, 15, 18 and 21a, Table 1, and Figure S1, ESM). It is interesting to note that the NBO analysis reveals for the CF_2 carbon a situation similar to that of the carbons involved in three-membered rings, with two hybrid orbitals $sp^{2.2}$ engaged in the endocyclic C–C bonds and two hybrid orbitals $sp^{4.2}$ engaged in the C–F bonds. As a result, although the CF_2 carbon geometry is closer to the tetrahedral one, it affects the six-membered ring like an unsaturated sp^2 carbon.

Simulations of the equilibrium in different solvents (benzene or methanol) of the allyl epoxide **5a**, **8a** and **9a** confirm the limited dependence of the conformer ratio on the dipole moment difference Δμ, when an *sp²-like* Y is present. In fact, while the ΔG for epoxide **9a** drops substantially, when the medium varies from vacuum to benzene and to methanol (entries 24a–c, Table 1), epoxides **5a** and **8a**, which has the largest Δμ value (+2.5 D), reveal only a modest shift of the conformational equilibrium toward the more polar conformer **A** (entries 10a–c and 21a–c, Table 1).

Looking for the structural parameters, which might be responsible for the equilibrium profile observed, we focused on the evaluation of torsional and electronic effects. While torsional tensions in conformers **A** and **B** are very similar in the case of saturated epoxides **2–3**, they become substantially different in the case of allyl epoxides **4–12**, mainly because of the strong preference of the unsaturated portion of the molecule for a planar geometry.

In the case of allyl epoxides **4–12**, the geometry of two conformers **A** and **B** can be visualized by considering the dihedral angles H–C(4)–C(5)–R^2 ($\boldsymbol{\theta_1}$) and C(5)–Y–C(1)–C(2) ($\boldsymbol{\theta_2}$), whose values are reported in Table 2 (see Scheme 3). The dihedral angles $\boldsymbol{\theta_1}$ and $\boldsymbol{\theta_2}$ change univocally during the conformational interconversion from conformer **A** to conformer **B**, and for this reason they are meaningful reaction coordinates. The dihedral angle $\boldsymbol{\theta_1}$ is obviously related to the torsional interactions along the bond between the saturated carbon bound to "Y" and the adjacent oxirane carbon; these interactions occour between the two pairs of bonds H–C(4)/C(5)–R^2 and O–C(4)/C(5)–R^1 and they are indicated by double-headed full-line arrows in Scheme 3.[3] This dihedral is approximately 52–72° in conformers **A** (staggered substituents), 26–30° in the **TS**s, and 3–9° in conformers **B** (eclipsed substituents). This torsional energy rises monotonically, moving along the reaction coordinate from **A** to **B**, and makes conformer **B** less stable with respect to conformer **A**, regardless of the nature of "Y". The dihedral angle $\boldsymbol{\theta_2}$ is related to the distance of the saturated carbon bound to the Y group from the plane containing "Y" and the double bond. As a consequence, $\boldsymbol{\theta_2}$ can be considered a measure of the ring flatness, and it is directly related to "ring strain" (angular tension + torsional tensions, due to the eclipsed bonds), which is maximum when its value approaches 0°. The dihedral $\boldsymbol{\theta_2}$ has about the same absolute value ($|\boldsymbol{\theta_2}|$ approximately 20°–43°) and the opposite sign in conformers **A** and **B**, and reaches the 0 value in proximity of the **TS** ($|\boldsymbol{\theta_2}|$=5°–10°) (Table 2 and Scheme 3).

The $\Delta G^{\ddagger}$ for **A** and **B** interconversion decreases as the Y hybridization turns from sp^3 into sp^2 (Table 1) because less "work" is required to get to the **TS**: the highest $\Delta G^{\ddagger}$ are associated with derivatives in which **A** and **B** have largest $|\boldsymbol{\theta_2}|$ value (epoxides **4a** and **9a**, entries 7 and 24a, Table 1 and entries 1–3 and 16–18, Table 2) and the lowest $\Delta G^{\ddagger}$ correspond to derivatives bearing an sp^2-*like* Y group (epoxides **5a** and **6a**, entries 10a and 15, Table 1 and 4–9, Table 2). The presence of an sp^2-*like* group substantially lowers the "ring strain" difference between the **TS** and conformers **A** and **B**, not only by an obvious reduction in the "angular tension" difference, but also by a lower

[3] The eclipsing (or staggering) of H–C(4)/C(5)-R^2 bonds necessarily determines the eclipsing (or staggering) of O–C(4)/C(5)-R^1 bonds. The value of the dihedral angle O–C(4)-C(5)-R^1 in conformer **B** is about 20–25°, but it is known that the bond critical point (BCP) in the bond path, for three-membered rings, is deviated from the bond axis by about the same amount.

Table 2 MP2/6-31+G(d) $|\boldsymbol{\theta_1}|$, $|\boldsymbol{\theta_2}|$ (degrees), C(3)–O and C(4)–O (Å) values in epoxides **4a–12a**

Entry[a]	Struct.	$\lvert\boldsymbol{\theta_1}\rvert$	$\lvert\boldsymbol{\theta_2}\rvert$	C(3)–O	C(4)–O
1	**4a-A**	63.4	33.6	1.469	1.443
2	**4a-TS**	26.0	8.3	1.465	1.450
3	**4a-B**	3.0	33.1	1.460	1.454
4	**5a-A**	56.6	23.6	1.480	1.434
5	**5a-TS**	26.0	7.9	1.469	1.445
6	**5a-B**	5.7	23.6	1.461	1.451
7	**6a-A**	54.2	25.8	1.485	1.435
8	**6a-TS**	28.7	9.9	1.482	1.441
9	**6a-B**	6.4	27.0	1.471	1.448
10	**7a-A**	63.5	26.2	1.472	1.434
11	**7a-TS**	26.9	5.4	1.469	1.442
12	**7a-B**	8.8	27.4	1.462	1.451
13	**8a-A**	60.0	26.8	1.464	1.438
14	**8a-TS**	30.5	7.6	1.461	1.446
15	**8a-B**	2.8	33.9	1.458	1.452
16	**9a-A**	71.8	43.4	1.468	1.437
17	**9a-TS**	29.2	10.5	1.455	1.436
18	**9a-B**	2.9	37.5	1.446	1.440
19	**10a-A**	56.2	20.1	1.465	1.441
20	**11a-A**	52.0	12.0	1.460	1.446
21	**12a-A**	56.2	22.4	1.477	1.435

[a] No significant differences in the geometrical parameters are found for epoxides **4b,c–12b,c**

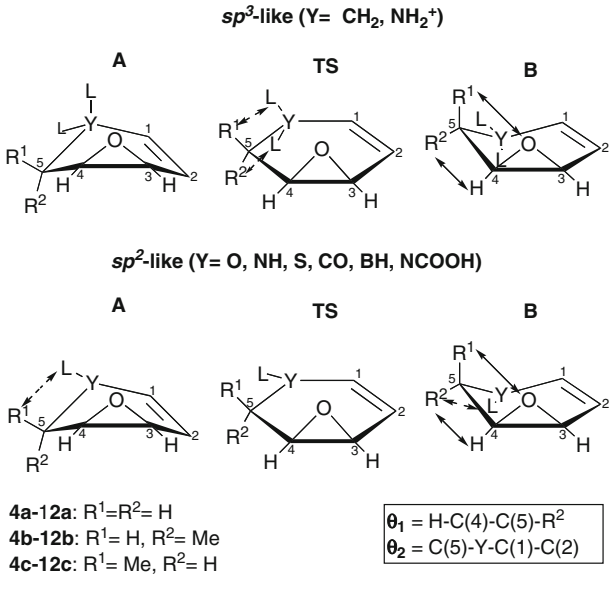

Scheme 3 Relevant torsional interactions affecting the conformational equilibrium, depending on the nature of the Y group

increase in the overall torsional tension, when the system reaches the **TS**. In Scheme 3, the double-headed dashed-line arrows show the two most important torsional tensions affected by the nature of "Y", which are those arising from the interactions of substituents at C(5) with the substituents and/or lone pair at "Y". With an sp^3-*like* Y group, both substituents at C(5) interact with the Y group more strongly in **TS** than in the minima, whereas with an sp^2-*like* Y group, only one substituent at C(5) interacts with "Y" in the minima (the possible second "substituent L" is a lone pair in the *p* orbital strongly interacting with the double bond, and not represented in Scheme 3) and the interaction is very weak in the **TS**.

The endocyclic sp^2 atom Y group can also affect the conformational profile by means of a resonance effect, which favors a flatter structure because of a better bonding-antibonding orbital interaction. The resonance effect between different Y groups and the double bond were evaluated in terms of the delocalization energy (E_2) calculated by the second-order investigation of the Fock matrix in the NBO analysis. These values are reported in Table 3, and the corresponding resonance structure is presented in Scheme 4: structures II and III correspond to the conjugative effect (mainly present when Y=O, NH, S, CO, BH and NCOOH); structures VI and VII correspond to the hyperconjugative effect (mainly present when Y=CH_2, CF_2 and NH_2^+). The larger values of E_2 are obviously found in general when a conjugative and no hyperconjugative effect takes place, which happens when an sp^2-*like* Y is present (entries 4–12 and 28–30, Table 3). Table 3 shows that the E_2 is generally higher for the **TS** than for minima (conformers **A** and **B**), and about the same for the two minima; as a consequence, the main effect of the resonance is to lower the $\Delta G^{\ddagger}$. The stronger the resonance effect (large E_2 values), the stronger the effect on the lowering barrier. It is interesting to note that electron-donating atoms and electron-deficient atoms have the same effect.

Epoxide **8a** (Y=CF_2) presents a special situation: the more substantial hyperconjugative effect of the CF_2 group (compared with the CH_2 and NH_2^+ group), due also to the presence of the additional interaction corresponding to the resonance structure VIII, determines an almost sp^2-*like* hybridization of the orbitals engaged in the endocyclic bonds (entries 13–21, Table 3). For this reason, the ΔG value for **8a** is closer to that of **7a** (Y=S) than to the corresponding values of epoxides **4a** (Y=CH_2) and **9a** (Y=NH_2^+) (entries 7, 18, 21a and 24a, Table 1). However, the absence of an orbital *p* (as in the case of epoxides **5a**–**7a** and **11a**, Y=O, NH, S, BH) or π system (as in the case of epoxides **10a** and **12a**, Y=CO, NCOOH) strongly interacting with the endocyclic double bond [C(1)=C(2)], makes the torsional interactions of substituents at C(5) with the CF_2 intermediate between an sp^2 and sp^3 situation. As a consequence, the $\Delta E^{\ddagger}$ and $\Delta G^{\ddagger}$ values found for epoxides **8** are intermediate between the corresponding ones calculated for epoxides **4** (Y=CH_2) and epoxides **5**–**7** (Y=O, NH, S) (entries 7–9, 10a,11a, 15,16, 18–21a, 22 and 23, Table 1).

Factors affecting the conformational profile can combine in such a way that no minimum energy corresponding to conformer **B** is found. This is the case with the flattest epoxides **10a**–**12a** (clear sp^2 Y group hybridization), in which the stability of conformer **B** is reduced with respect to the structure corresponding to "**TS**" (entries 27, 30 and

Table 3 MP2/6-31+G(d) NBO analysis: Y group-double bond interactions (kcal/mol) in epoxides **4a**–**12a**

Entry	Structure	Y	Donor–acceptor	E_2^a (kcal/mol)	Resonance structure
1	**4A**	CH_2	σ (C–H)→π*	1.48, 6.10[b]	VII
2	**4-TS**		σ (C–H)→π*	6.72, 3.16[b]	VII
3	**4B**		σ (C–H)→π*	5.53, 1.76[b]	VII
4	**5A**	O	LP(O)→π*	39.01	III
5	**5-TS**		LP(O)→π*	44.89	III
6	**5B**		LP(O)→π*	39.45	III
7	**6A**	NH	LP(N)→π*	51.92	III
8	**6-TS**		LP(N)→π*	68.84	III
9	**6B**		LP(N)→π*	49.38	III
10	**7A**	S	LP(S)→π*	28.94	III
11	**7-TS**		LP(S)→π*	36.26	III
12	**7B**		LP(S)→π*	26.92	III
13	**8A**	CF_2	π →σ*(C–F)	10.53, 3.40[b]	VI
14			σ (C–F)→π*	1.34, 0.53[b]	VII
15			LP(F)→π*	1.19	VIII
16	**8-TS**		π →σ*(C–F)	6.55, 8.61[b]	VI
17			σ (C–F)→π*	0.95, 1.51[b]	VII
18			LP(F)→π*	1.29, 0.88[b]	VIII
19	**8B**		π →σ*(C–F)	2.04, 10.76[b]	VI
20			σ (C–F)→π*	1.34	VII
21			LP(F)→π*	1.19	VIII
22	**9A**	NH_2^+	σ (N–H)→π*	3.34	VII
23			π →σ*(N–H)	2.15	VI
24	**9-TS**		σ (N–H)→π*	2.33, 3.68[b]	VII
25			π →σ*(N–H)	2.71, 1.98[b]	VI
26	**9B**		σ (N–H)→π*	0.70, 3.40[b]	VII
27			π →σ*(N–H)	3.04	VI
28	**10A**	C=O	π →π*(C=O)	25.56	II
29	**11A**	BH	π→LP*(B)	32.87	II
30	**12A**	NCOOH	π(C_-_-N)→π*	37.12	III

[a] Delocalization energy calculated by second-order investigation of the Fock matrix

[b] The two values resulted from the two chemically non-equivalent contributions from above and below the plane

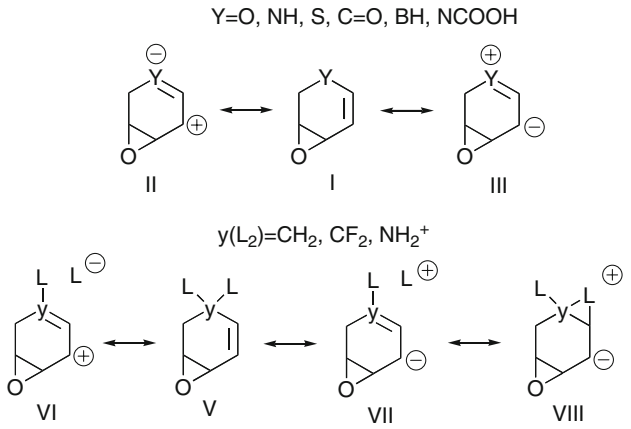

Scheme 4 Resonance structures corresponding to the Y group-double bond interactions shown in Table 3

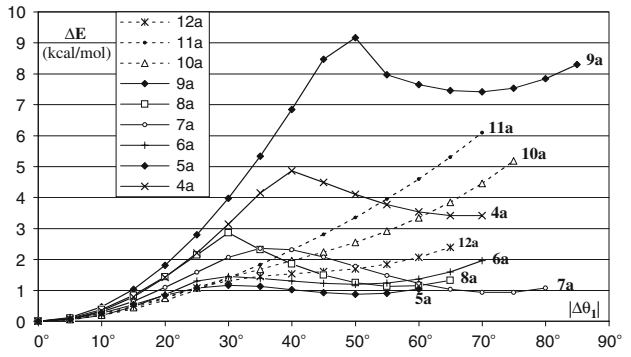

Fig. 2 MP2/6-31+G(d) ΔE (kcal/mol) scan on the $|\Delta\theta_1|$ (degrees) from conformer **A** (origin) to conformer **B**, when present, in epoxides **4a–12a**

33, Table 1 and 19–21, Table 2). In other words, when $\Delta E^{\ddagger}$ becomes lower than ΔE, values that can be approximately extrapolated from the conformational profile for epoxides **10a–12a** shown in Fig. 2, **B** may not be present in the conformational equilibrium.[4]

The presence of a side chain (methyl group) in epoxides **4b–12b** and **4c–12c** modifies the conformational equilibrium mainly by the steric effect. The data of Table 1 show that while *trans* substitution (epoxides **4b–9b**) lowers the ΔG between conformers **A** and **B**, *cis* substitution (epoxides **4c–9c**) enhances the ΔG between conformers **A** and **B** compared with the corresponding unsubstituted epoxides (**4a–9a**). The free energy of conformer **A** of the *trans* diastereoisomer is generally higher (epoxides **4–9**) or about the same (epoxides **10–11**) compared with the conformer **A** of the corresponding *cis* diastereoisomer, as indicated by the free energy differences ΔG(**A**) shown in Table 4: ΔG(**A**) is highest for epoxides **6** and **5** (entries 2 and 3) and negligible for the flattest epoxides **10** and **11** (entries 7 and 8). On the other hand, the free energy of conformer **B** is lower in the *trans* diastereoisomer than in the corresponding *cis* diastereoisomer, and this energy difference ΔG(**B**) is always higher than the ΔG(**A**) (Table 4). The reason for this is that the C(4)–O/C(5)–H eclipsing, present in the conformer **B** of unsubstituted epoxides **4a–9a** and *trans* epoxides **4b–9b**, is replaced in the conformer **B** of *cis* epoxides by the more disfavored C(4)–O/C(5)–CH_3 eclipsing (Scheme 3). Moreover, this eclipsing is absent in the corresponding **TS**s, and for this reason the presence of the methyl group in the *cis* diastereoisomers enhances the energy of conformer **B** more than the energy of **TS** with respect to the corresponding unsubstituted or *trans* epoxides. Generally, while the *trans* substitution enhances the $\Delta E^{\ddagger}$–ΔE value (the depth of the minimum corresponding to conformer **B**), the *cis* substitution lowers the $\Delta E^{\ddagger}$–ΔE, with respect to the corresponding unsubstituted epoxide (Table 4). In other words, the existence of the conformer **B** as a minimum energy is more likely with *trans* substituted epoxides and less likely with *cis* substituted ones. When the $\Delta E^{\ddagger}$–ΔE value calculated for unsubstituted epoxides is very small, as in the case of epoxides **5a** and **6a** (about 0.5 kcal/mol, entries 2 and 3, Table 4), the conformer **B** of the corresponding substituted *cis* epoxides is not a minimum energy, and only conformer **A** is found in the equilibrium (entries 12 and 17, Table 1). Only in the case of epoxides **8** is the $\Delta E^{\ddagger}$–ΔE value higher for epoxide *cis* **8c** with respect to the unsubstituted epoxide **8a**, because of the above-discussed intermediate nature between sp^2 and sp^3 of the CF_2 group (entry 5, Table 4). In this case, the methyl group in the **8b-TS** and **8c-TS** is eclipsed with the C–F bond (Scheme 3) and as a consequence, the $\Delta E^{\ddagger}$ value of both epoxides **8b** and **8c** is higher with respect to the $\Delta E^{\ddagger}$ value of epoxides **5b–7b** and **7c**.

In the flattest *trans* epoxides **10b–11b**, the effect of *trans* substitution is not so strong as to make positive the corresponding $\Delta E^{\ddagger}$–ΔE (negative in the related unsubstituted epoxide **10a** and **11a**);[4] as a consequence, conformer **A** only is present in the equilibrium of both *trans* epoxides **10b–11b** and *cis* epoxides **10c–11c** (entries 28–29 and 31–32, Table 1).

The only exception to these generalizations is represented by epoxides **12b** and **12c** (Y=NCOOH), where the equilibrium is controlled by the $A^{1,3}$ strain [34, 35]. In these epoxides, the eclipsing C(5)–Me/N–COOH makes the conformer where it occurs (**B** in **12b** and **A** in **12c**) so disfavored that epoxide **12b** and **12c** exist only as

[4] In the case of epoxides **10–12**, and in all cases in which no minimum energy **B**-type conformer **B** and related **TS** are found, ΔE and $\Delta E^{\ddagger}$ can be approximately extrapolated by means of $|\theta_1|$ values for conformer **A** ($|\theta_1|_A$) and by considering that $|\theta_1|$ value for conformer **B** ($|\theta_1|_B$) and **TS** ($|\theta_1|_{TS}$) is about 3–9° and 26–30°, respectively (Table 2). The $|\theta_1|_A$-$|\theta_1|_B$ and $|\theta_1|_A$-$|\theta_1|_{TS}$ differences give the $|\Delta\theta_1|$ values to be used in Fig. 2 in order to locate, in the conformational profile, the geometry corresponding to conformer **B** and **TS**, respectively.

Table 4 $\Delta G(\mathbf{A})$, $\Delta G(\mathbf{B})$ for epoxides *trans* and *cis* **4b,c–12b,c** and $\Delta E^{\ddagger}$–ΔE for epoxides **4–12**

Entry	Structure	Y	$\Delta G(\mathbf{A})$[a]	$\Delta G(\mathbf{B})$[b]	$\Delta Ea^{\ddagger}$–ΔEa[c]	$\Delta Eb^{\ddagger}$–ΔEb[d]	$\Delta Ec^{\ddagger}$–ΔEc[e]
1	**4**	CH_2	+0.46	−1.03	+1.74	+2.76	+1.43
2	**5**	O	+1.13	–	+0.60	+1.24	<0[f]
3	**6**	NH	+1.29	–	+0.32	+0.59	<0[f]
4	**7**	S	+0.38	−1.06	+1.77	+2.64	+1.06
5	**8**	CF_2	+0.36	−0.65	+2.19	+4.07	+3.13
6	**9**	NH_2^+	+0.50	−0.51	+2.06	+2.98	+1.75
7	**10**	BH	−0.12	–	<0[f]	<0[f]	<0[f]
8	**11**	C=O	+0.14	–	<0[f]	<0[f]	<0[f]
9	**12**	NCOOH	–	–	<0[f]	<0[f]	<0[f]

[a] G(**xb-A**)–G(**xc-A**)

[b] G(**xb-B**)–G(**xc-B**)

[c] Unsubstituted epoxide

[d] Epoxide *trans*

[e] Epoxide *cis*

[f] Extrapolated value

conformer **A** and **B**, respectively, in which such eclipsing is absent (see Scheme 3 and entries 34–35, Table 1).

Calculations of equilibria in different solvents (benzene and methanol) on epoxides **5b** and **5c** confirmed that epoxide **5c** exists only as conformer **A**, regardless of the nature of the solvent, and indicated for epoxide **5b** a low dependence of the conformational equilibrium on the dipole moment difference Δμ (entries 11a–c and 12, Table 1).

The replacement of the methyl group with the more polar $-CH_2OMe$ group (epoxides **5d** and **5e**) does not substantially affect the overall conformational population (entries 13a–c and 14, Table 1). However, the presence of the $-CH_2OMe$ group makes the conformer population of **5d** a little more sensitive than **5b** to the polarity of the solvent, which favors conformation **A** (entries 11a–c and 13a–c, Table 1).

2.1 Prediction of reactivity in the oxirane ring-opening for epoxides **4–12**

An important reactivity of allyl epoxides is the addition of nucleophiles. Experimental results have shown that carbocylic epoxide analogs of **4a** are stable and isolable [30], whereas heterocycle epoxides related to **5a** (the glycal-derived epoxides **1α** and **1β** [2–4], Scheme 1) or **12a** (the *N*-Cbz-imino glycal-derived epoxides **13α** and **13β**, Scheme 5 [5]), are too reactive to be isolated. However, while **1α** and **1β** and epoxide **13α** must be allowed to react shortly after they have been generated in situ, a solution of epoxide **13β** has a shelf life of 2 days at –20° (see Scheme 5).

Searching for a molecular paramenter which could be related to the reactivity, the elongation of the allyl C(3)–O bond appeared to be an interesting candidate, because it is the bond which is broken in the ring-opening process. Table 2 shows the values of the C(3)–O bond for conformers **A** and **B** and related **TS** corresponding to unsubstituted epoxides **4a–12a** only, but no significant differences are found when the side chain (methyl group) is present in position 5 (epoxides **4b,c–12b,c**). The comparison of the homogeneous values corresponding to conformers **A** reveals that the elongation of the C(3)–O bond follows the donating ability of the Y group quantified by the E_2 of the Y/double bond interaction: $Y=CH_2 < Y=S < Y=NCOOH < Y=O < Y=NH$ (entries 1, 4, 7, 10, 21, Table 2 and 1, 4, 7, 10, 30, Table 3). On the basis of these data, it is possible to predict that epoxides **8a–11a** ($Y=CF_2$, NH_2^+, CO and BH), in which an electron-deficient Y group is present, should be less reactive in the opening process than carbocyclic epoxide **4a**, taken as a reference compound, with epoxide **11a** being the least

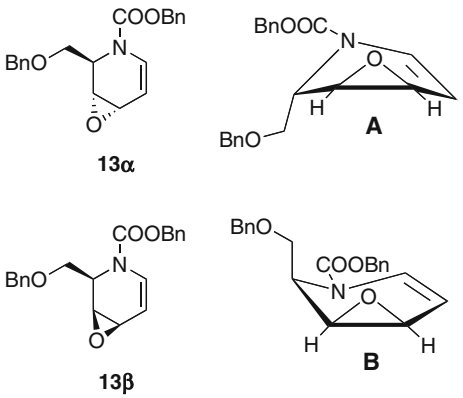

Scheme 5 Single minimum energy conformations of epoxides **13α** and **13β**

reactive one (entry 20, Table 2). On the other hand, epoxides bearing an electron-donating Y group (epoxides **5a**–**7a** and **12a**) should be more reactive than epoxide **4a**, and among them, epoxides **5a** and **6a** should be the most reactive ones, in accordance with experimental evidence (entries 4 and 7, Table 2).

As a general observation, conformers **A** exhibit a longer C(3)–O bond than corresponding conformers **B**. As the C(3)–O bond becomes longer, the C(4)–O bond becomes shorter during the **A** to **B** interconversion, with the consequent reduction of the asymmetry of the oxirane ring (see Table 2). We thus postulated that the opening process of epoxides **4**–**12** should take place when the compound is in the **A** conformation. This hypothesis explains the different stability and reactivity in the oxirane nucleophilic ring-opening process of epoxides **13α** and **13β** [5], for which only one minimum energy conformation was found: conformer **A** for *trans* epoxide **13α** (similar to epoxide **12b**) and conformer **B** for *cis* epoxide **13β** similar to epoxide **12c** (Scheme 5). We also performed a scan on the PES along the values of angle C(3)–C(4)–O (a measure of the oxirane ring-opening degree) with the conformer **5a**-**B** as the starting geometry: when the C(3)–C(4)–O angle reaches the value of about 70°, a conformational change to conformer **A** takes place, with an associated reduction in the potential energy.

The reason for the larger asymmetry of the oxirane ring in conformer **A** is an overall larger interaction of the σ(C(3)–O) orbital, and at the same time, an overall smaller interaction of the σ(C(4)–O) with several σ^* bonds in conformer **A** with respect to conformer **B**: the ΔE_2 between the two conformers **A** and **B** relative to the delocalization of the C(3)–O bond in the σ^* bonds is about 2–3 kcal/mol. The ΔE_2 between conformers **A** and **B** calculated for the interaction $\pi \rightarrow \sigma^*$(C(3)–O) is only 1 kcal/mol, but in this case, it is conformer **B** that presents the higher E_2 (Table S7, ESM), and for this reason this interaction does not explain the longer C(3)–O bond found in conformer **A**.

3 Comparison of different calculation methods

In the case of saturated epoxides **2**–**3**, the results obtained with B3LYP are very similar to those obtained using MP2, particularly for cyclohexene oxide **2a** [29], **2b** and **2c**. As regards the allyl epoxides **4**–**12**, the geometries obtained by DFT generally show a flatter ring, and the corresponding $\Delta G(\Delta E)$ and $\Delta G^{\ddagger}(\Delta E^{\ddagger})$ are somewhat lower than the ones calculated by MP2 (Table S5, ESM). However, this energy difference cannot be attributed to the increase in the cycle flatness, because the results obtained by performing an MP2 Single Point calculation on the previously B3LYP optimized structures are very similar to those obtained by performing the complete and substantially more CPU-expensive MP2 optimization (Table S4, ESM). Furthermore, a larger basis set [6–311++(d,p)] does not have any influence on the B3LYP results. The difference is intrinsic to the methodology, and in particular to the method used for the calculation of the delocalization energies. In fact, the E_2 values obtained in the NBO analysis using B3LYP are somewhat different from the corresponding ones obtained by MP2. The E_2 values corresponding to the interactions between the Y group and the double bond, as well as the ΔE_2 values between the minima (conformers **A** and **B**) and the corresponding **TS**, are generally lower if B3LYP is used.

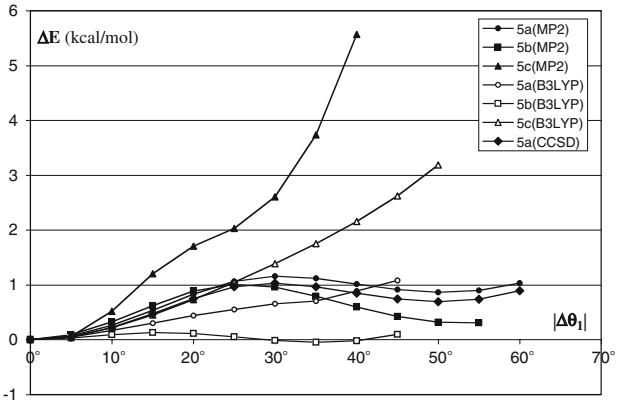

Fig. 3 B3LYP, MP2 and CCSD ΔE (kcal/mol) scan on the $|\Delta\theta_1|$ (degree) from the more stable conformer **A** (origin) to the less stable conformer **B**, when present, for epoxides **5a**–**c**

The shape of the $|\Delta\theta_1|$ scan curves is generally flatter, and the potential holes, corresponding to the minima, are less deep, if B3LYP is used. This determines the absence of the minimum corresponding to conformer **B** also in epoxides **4c**, **5a**, **6a** and **7c**, contrary to MP2 findings (entries 9, 10a–c, 13 and 18, Table S4, and entries 9, 10a–c, 15 and 20, Table S5, ESM). The different shape of the scan on $|\Delta\theta_1|$, using both MP2 and B3LYP, for epoxides **5a**–**c** is shown in Fig. 3. The charts corresponding to the remaining saturated and allyl epoxides (**2**–**4** and **6**–**12**) and the comparison of the MP2 and B3LYP energies for these epoxides may be found in Figure S2 and Tables S4, S5, respectively (ESM).

As no experimental data for allyl epoxides **4**–**12** is available for comparison with our theoretical results, we decided to perform calculations at a higher level of theory, in particular MP4 and CCSD, to see whether MP2 or B3LYP is in better agreement with these presumably more accurate calculations. The CCSD level of theory, in particular, has been shown to be very reliable for computing energies for a large number of systems, and without experimental data, this is the best comparison available to us.[5] For this purpose, epoxide **5a**, in which a strong conjugative effect between the

[5] Generally, a larger basis set than 6–31+G(d) is employed in MP4 and CCSD calculations, but in this case it would have been too expensive from a computational point of view.

Table 5 ΔE and $\Delta E^{\ddagger}$(kcal/mol) of epoxide **5a** obtained by different calculation methods

Entry	Method	ΔE	$\Delta E^{\ddagger}$
1	MP2	+0.87	+1.16
2	MP4	+0.77[a]	+1.09[a]
3	CCSD	+0.69[a]	+1.02[a]
4	CCSD	+0.70	

[a] SP on the previously MP2 optimized geometries

double bond and the endocyclic oxygen is present, was chosen. The MP4 and CCSD results essentially confirm the geometries, energy differences, and NBO analysis obtained by MP2 calculations. Furthermore, the complete energetic profile, performed by CCSD ΔE scan on the $|\Delta\theta_1|$ for epoxide **5a**, turned out to be practically superimposable on the one obtained by MP2 calculation (Fig. 3). As CCSD, MP4 and MP2 are wave function-based methods, while B3LYP is a hybrid density functional method, it was not unexpected that CCSD, MP4 and MP2 gave results which are close to each other (Table 5).

4 Conclusions

In most cases of all epoxides derived from six-membered cyclic systems, two minimum energy conformations were found, which differ in the relative position of the Y group and the epoxy oxygen, with respect to a plane containing the epoxy ring carbons and the adjacent saturated endocyclic carbon: they may be on the same side (conformer **A**) or on opposite sides (conformer **B**).

While in the saturated cyclic epoxides **2–3**, the dipole moment and the steric interactions of the side chain (when present) are the principal factors influencing the conformational equilibrium, when the double bond is present (allyl epoxides **4–12**), except for the epoxides bearing an *sp^3-like* Y group, the ΔG is unvaried with respect to the dipole moment difference. The conformational profile (ΔG and $\Delta G^{\ddagger}$) of cyclic allyl epoxides depends rather on torsional tension factors and electronic interactions (electron-donating or electron-withdrawing effects) of the Y group with the double bond. Generally, conformer **A** is favored because of the greater torsional strain present in conformer **B**. The interconversion barrier ($\Delta G^{\ddagger}$) between conformers **A** and **B** decreases as the Y group hybridization turns from *sp^3-* into *sp^2-like* and, as a consequence, the absence of the less deep minimum corresponding to conformer **B** is more likely, as actually found in epoxides **10a–12a**.

The presence of a side chain (methyl group) in epoxides **4b–12b** and **4c–12c** modifies the conformational equilibrium mainly by its steric effects. Apart from epoxides **12b** and **12c**, in which a particular repulsive interaction ($A^{1,3}$ strain) is present between the side chain on C(5) and the Y group (NCOOH), the ΔG between conformers **A** and **B** is lowered by *trans* substitution (epoxides **4b–9b**) and enhanced by *cis* substitution (epoxides **4c–9c**) with respect to the corresponding unsubstituted epoxides (**4a–9a**). Generally, the existence of a conformer **B** as a minimum energy is more likely with *trans* substituted epoxides and less likely with *cis* substituted ones.

On the basis of the elongation of the allylic oxirane C(3)–O bond, the reactivity of epoxides **4–12** in the ring-opening process was predicted to depend on the electron-donating ability of the Y group: the more electron-donating the Y group is, the higher the reactivity and consequently the less stable the molecule is, in agreement with experimental evidence, obtained with carbocylic, oxygen and nitrogen allyl epoxides. As conformer **A** exhibits a larger C(3)–O bond length than conformer **B**, we postulated that the opening process should take place, when the compound is in the **A** conformation. This hypothesis explains the lower stability and reactivity of epoxides **13*β*** with respect to epoxide **13*α*** in the nucleophilic addition.

DFT and the perturbative MP2 method do not give substantially different results, particularly in the case of saturated epoxides **2–3**. The most substantial differences between different calculation methods adopted are found when the double bond is present in the cycle. In particular, the DFT-optimized structures are flatter and the DFT-calculated $\Delta G^{\ddagger}$ and $\Delta E^{\ddagger}$ are lower than found by MP2. This fact is responsible for the absence of minima corresponding to the less stable conformer **B**, in a larger number of epoxides.

Acknowledgments This work was supported by the Università di Pisa, the Ministero dell'Università e della Ricerca Scientifica (MIUR). P. C. gratefully acknowledges Merck Research Laboratories for generous financial support deriving from the 2005 ADP Chemistry Award. Dr Elio Napolitano is gratefully acknowledged for helpful discussions.

References

1. Olofsson B, Somfai P (2006) Vynil epoxides in organic synthesis. In: Yudin AK (ed) Aziridines and epoxides in organic synthesis. Wiley, Weinheim, pp 315–347
2. Di Bussolo V, Caselli M, Romano MR, Pineschi M, Crotti P (2004) J Org Chem 69:7383. doi:10.1021/jo0491152
3. Di Bussolo V, Caselli M, Romano MR, Pineschi M, Crotti P (2004) J Org Chem 69:8702. doi:10.1021/jo048981b
4. Di Bussolo V, Favero L, Romano MR, Pineschi M, Crotti P (2008) Tetrahedron 64:8188. doi:10.1016/j.tet.2008.06.039
5. Di Bussolo V, Fiasella A, Romano MR, Favero L, Pineschi M, Crotti P (2007) Org Lett 9:4479. doi:10.1021/ol701836a
6. Takhi M, Abdel-Rahman AAH, Schmidt RR (2001) Synlett 427 and references therein

7. Horita K, Sakurai Y, Nagasawa M, Yonemitsu O (1997) Chem Pharm Bull Tokyo 45:1558
8. Linde RGII, Egbertson M, Coleman RS, Jones AB, Danishefsky SJ (1990) J Org Chem 55:2771. doi:10.1021/jo00296a040
9. Danishefsky SJ, DeNinno S, Lartey P (1987) J Am Chem Soc 109:2082. doi:10.1021/ja00241a028
10. Frisch MJ, Trucks GW, Schlegel HB, Scuseria GE, Robb MA, Cheeseman JR, Montgomery JA Jr, Vreven T, Kudin KN, Burant JC, Millam JM, Iyengar SS, Tomasi J, Barone V, Mennucci B, Cossi M, Scalmani G, Rega N, Petersson GA, Nakatsuji H, Hada M, Ehara M, Toyota K, Fukuda R, Hasegawa J, Ishida M, Nakajima T, Honda Y, Kitao O, Nakai H, Klene M, Li X, Knox JE, Hratchian HP, Cross JB, Bakken V, Adamo C, Jaramillo J, Gomperts R, Stratmann RE, Yazyev O, Austin AJ, Cammi R, Pomelli C, Ochterski JW, Ayala PY, Morokuma K, Voth GA, Salvador P, Dannenberg JJ, Zakrzewski VG, Dapprich S, Daniels AD, Strain MC, Farkas O, Malick DK, Rabuck AD, Raghavachari K, Foresman JB, Ortiz JV, Cui Q, Baboul AG, Clifford S, Cioslowski J, Stefanov BB, Liu G, Liashenko A, Piskorz P, Komaromi I, Martin RL, Fox DJ, Keith T, Al-Laham MA, Peng CY, Nanayakkara A, Challacombe M, Gill PMW, Johnson B, Chen W, Wong MW, Gonzalez C, Pople JA (2003) Gaussian 03, Revision A.1. Gaussian, Pittsburgh
11. Moller C, Plesset MS (1934) Phys Rev 46:618. doi:10.1103/PhysRev.46.618
12. Head-Gordon M, Pople JA, Frisch M (1988) Chem Phys Lett 153:503. doi:10.1016/0009-2614(88)85250-3
13. Saebo S, Almlof J (1989) Chem Phys Lett 154:83. doi:10.1016/0009-2614(89)87442-1
14. Head-Gordon M, Pople JA, Frisch M (1990) Chem Phys Lett 166:281. doi:10.1016/0009-2614(90)80030-H
15. Head-Gordon M, Head-Gordon T (1994) Chem Phys Lett 220:122. doi:10.1016/0009-2614(94)00116-2
16. Ziegler T (1991) Chem Rev 91:651 and references therein. doi:10.1021/cr00005a001
17. Petersson GA, Al-Laham MA (1991) J Chem Phys 94:6081. doi:10.1063/1.460447
18. Schlegel HB (1982) J Comput Chem 3:214. doi:10.1002/jcc.540030212
19. Krishnan R, Pople JA (1978) Int J Quantum Chem 14:91. doi:10.1002/qua.560140109
20. Scuseria GE, Janssen CL, Schaefer HFIII (1988) J Chem Phys 89:7382. doi:10.1063/1.455269
21. Scuseria GE, Schaefer HFIII (1989) J Chem Phys 90:3700. doi:10.1063/1.455827
22. McQuarrie DA (1974) Statistical thermodynamics. Harper and Row, New York
23. Ben-Naim A (1987) Solvation thermodynamics. Plenum, New York
24. Tomasi J, Persico M (1994) Chem Rev 94:2027. doi:10.1021/cr00031a013
25. Cossi M, Barone V, Cammi R, Tomasi J (1996) J Chem Phys Lett 255:327. doi:10.1016/0009-2614(96)00349-1
26. Cances E, Mennucci B, Tomasi J (1997) J Chem Phys 107:3032. doi:10.1063/1.474659
27. Cossi M, Barone V, Mennucci B, Tomasi J (1998) Chem Phys Lett 286:253. doi:10.1016/S0009-2614(98)00106-7
28. Mennucci B, Cammi R, Tomasi J (1998) J Chem Phys 109:2798. doi:10.1063/1.476878
29. Pawar DM, Noe EA (1998) J Am Chem Soc 120:1485. doi:10.1021/ja972493m
30. Murray R, Singh M, Williams BL, Moncrieff HM (1996) J Org Chem 61:1830 and references therein. doi:10.1021/jo951864j
31. Catelani G, Monti L, Tognetti P (1981) Carbohydr Res 97:189. doi:10.1016/S0008-6215(00)80665-5
32. Bianucci AM, Catelani G, Colonna F, Monti L (1985) Carbohydr Res 140:144. doi:10.1016/0008-6215(85)85059-X
33. Millet R, Alexakis A (2007) Synlett 435 and references therein
34. Craig D, McCague R, Potter GA, Williams MRV (1998) Synlett 55. doi:10.1055/s-1998-1566
35. Andreu R, Garìn J, Orduna J, Saviròn M, Uriel S (1995) Tetrahedron Lett 36:4319. doi:10.1016/0040-4039(95)00749-3